Resilient Information Architecture Platform for Smart Systems (RIAPS): Case Study for Distributed Apparent Power Control

Yuhua Du, Hao Tu, Srdjan Lukic, David Lubkeman
FREEDM Systems Center
North Carolina State University
Raleigh, NC, USA
{ydu7, htu, smlukic, dllubkem} @ncsu.edu

Abhishek Dubey, Gabor Karsai
Institute for Software Integrated Systems
Vanderbilt University
Nashiville, TN, USA
{abhishek.dubey, gabor.karsai} @vanderbilt.edu

***Abstract*—Maintaining voltage and frequency stability in an islanded microgrid is challenging, due to the low system inertia. In addition, islanded microgrids have limited generation capability, requiring that all DGs contribute proportionally to meet the system power consumption. This paper proposes a distributed control algorithm for optimal apparent power utilization in islanded microgrids. The developed algorithm improves system apparent power utilization by maintaining proportional power sharing among DGs. A decentralized platform called Resilient Information Architecture Platform for Smart Systems (RIAPS) is introduced that runs on processors embedded within the DGs. The proposed algorithm is fully implemented in RIAPS platform and validated on a real-time microgrid testbed.**

Keywords*—Microgrid, Optimal apparent power utilization, RIAPS platform, Distributed algorithm, Hierarchical control.

I. Introduction

Hierarchical control is used to manage steady-state and dynamic performance of islanded microgrids [1]. Primary control uses droop control to automatically stabilize the islanded microgrid. Droop control reacts on local state measurements, and results in steady state deviations in system frequency and voltage. Secondary control removes the steady state errors in system frequency and voltage while achieving additional objectives like power sharing or harmonic compensation [2].

Most commercial secondary control implementations utilize a microgrid centralized controller (MCC) [3], using a master-slave control strategy. All the controllable resources require direct communication links to the centralized controller, which presents a single point of failure and possibly a slow system response if the communication channels are overtasked. On the whole, centralized control reduces system reliability and does not support DG plug-and-play functionality [4], [5]. Decentralized control approach is favored to obviate the need for information routing to a single point [6]. Distributed control approach equips all controllable resources with decision making and plug-and play capability, thus eliminating a single point of failure.

Distributed secondary controllers for islanded microgrids, aiming to achieve proportional power sharing were presented in [7]–[11]. Generally speaking, active power sharing control can be achieved by shifting the droop curve, where different algorithms result in different shifting patterns [7], [8]. Distributed reactive power sharing control can be achieved by shifting the primary droop curve [9] or by implementing virtual impedance [10]. Most algorithms, however, consider active and reactive power control separately while ignoring the apparent power flow within the system. In a balanced islanded microgrid, the total apparent power generation does not necessarily need to be equal to the total apparent power consumption [11], which would potentially introduce circulating reactive power flow to the system. Circulating power flow among paralleled converters would not only limit the total system capacity but also jeopardize system operational security [12]. Such circulating power could be suppressed by minimizing the difference between apparent power generation and consumption.

Despite the vast literature on distributed microgrid control, little effort has been made to develop a platform to provide key capabilities to build and realize microgrid control applications. Such a platform should allow for straightforward implementation of complex distributed applications, while supporting time synchronization among all nodes and distributed co-ordination and management of concurrency. The platform should be able to handle microgrid operations with interacting software programs, deploy algorithm on devices across the network and solve problems collaboratively.

In this paper, we present an overview of Resilient Information Architecture Platform for Smart Systems (RIAPS) platform designed to address the needs of deploying distributed microgrid applications. A distributed apparent power control algorithm is proposed for islanded microgrid to achieve optimal apparent power utilization under secondary hierarchical control. The proposed algorithm imporves on the work presented in [7], [8] by ensuring that the apparent power is shared proportionally by each DG. The proposed algorithm is fully implemented in the RIAPS platform and validated on a real-time hardware-in-the-loop testbed.

II. RIAPS System Architecture Overview

Microgrids contain multiple DGs and loads controlled by different entities, which may have disparate operational objectives (eg. prosumers). Microgrids are, therefore, ideally suited for distributed control solutions, which can remove single point of failures. Creating distributed applications, however,

978-1-5386-5583-2/18/$31.00

poses a number of challenges. Not only does it require a distributed control algorithm, it also requires robust communication, support for time synchronization and distributed coordination and management of concurrency. Without these services the distributed control systems may fail if these orthogonal services are not functioning properly [13].

To handle these challenges our team is developing the Resilient Information Architecture Platform for Smart Grid (RIAPS). RIAPS is a distributed middleware platform that provides core services, language abstractions and modularization constructs that enables system integrators to quickly assemble a large distributed implementation of a novel distributed control algorithm. The platform delivers services that are critical to microgrid control (details are available in [14]).

Specifically, 1) The discovery and deployment mechanism ensures the control algorithm is distributed from a single node to the entire system. 2) The messaging middleware, ZeroMQ, facilitates information exchange between the RIAPS nodes. Messaging schemes such as request-reply and publish-subscribe can be easily implemented. 3) Communication protocols interfacing RIAPS nodes with outside world are implemented as library component. Examples include but not limited to Modbus and IEEE C37.118.2 synchrophasor data transfer protocol. 4) Time synchronization between different RIAPS nodes is maintained.

In RIAPS, distributed algorithms are called applications, described by two models. The first model is a **.riaps** file that describes the actors used in the application. One application can have several actors. Each actor realizes an abstract function such as control or data logging. Actors consist of components. Components as the basic unit represent the physical functions such as measurement sensing or calculation. Each component can have several kinds of ports to support its function. For example a timer port which wakes up every time step is usually implemented in an algorithm calculation component. Other ports, used in this paper, include publish and subscribe port to publish and subscribe messages, respectively. Message is defined by RIAPS as structured information exchanged between nodes. Each subscribe port and publish port are associated with a message with a specific topic. When one publish port publishes a message, the subscribe port that subscribes that message will receive it automatically. This routing of messages is handled by RIAPS discovery service. The construction of a RIAPS component is shown in Fig. 1.

The second model of an application is a **.depl** file that describes how actors are deployed onto physical RIAPS nodes. Instances of an actor can be deployed to many physical nodes, allowing the distributed algorithm to be efficiently deployed.

III. Problem Formulation

Droop characteristics, representing a predominantly inductive system, implement the microgrid primary control in $i-th$ droop-controlled DG:

$$\omega_i = \omega^* - m_i(P_i - P_i^*) + \Omega_i' \tag{1a}$$

$$E_i = E^* - n_i(Q_i - Q_i^*) + e_i \tag{1b}$$

where ω_i and E_i represent the measured DG frequency and voltage; ω^* and E^* represent nominal frequency and voltage;

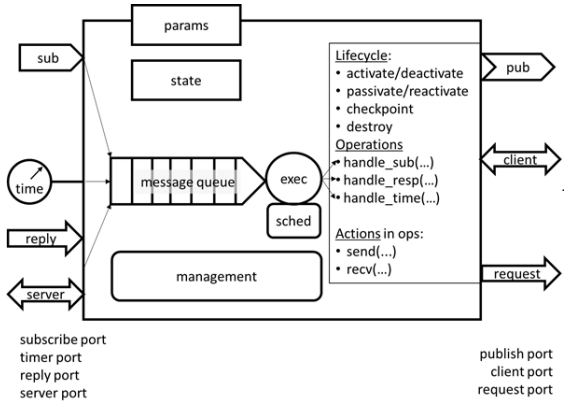

Fig. 1: RIAPS component structure

P_i and Q_i represent measured active and reactive power output; P_i^* and Q_i^* represent active and reactive power output reference when DG operates under nominal frequency and voltage; m_i and n_i represent static droop gains and are usually designed to be inversely proportional to DG's rated apparent power: $m_i, n_i \propto \frac{1}{S_{rated,i}}$. Under droop control, any power mismatch within the system would lead to steady state error in system frequency and voltage [9]. Secondary control is introduced to eliminate such deviations by shifting the droop curves by controlling paramters Ω_i' and e_i.

Droop control ensures that all DGs respond in proportion to their capacity to compensate for any power imbalance, ensuring that in a balanced islanded microgrid, the vector sum of apparent power generated by each DG, $\vec{S_G}$, would always be equal to total apparent power consumption $\vec{S_L}$ ($\vec{S_G} = \vec{S_L}$). However, the algebraic sum of apparent power generation is determined by the power factor of each DG, which is different for each secondary control strategy. Without proper control, it is possible that the sum of generated apparent power is greater than the demand ($\left|\vec{S_G}\right| > \left|\vec{S_L}\right|$). In such cases, the generated apparent power is not utilized optimally, resulting in circulating power in the system. In order to fully utilize the generated apparent power ($\left|\vec{S_G}\right| = \left|\vec{S_L}\right|$) while keeping a reasonable power sharing ratio among the DGs, following conditions should be met for $i = 1$ to n:

$$\frac{P_i}{Q_i} = \frac{P_j}{Q_j} \tag{2a}$$

$$\frac{P_i}{P_j} = \frac{Q_i}{Q_j} = \frac{S_{rated,i}}{S_{rated,j}} \tag{2b}$$

where P_i and Q_i represent the active/reactive power output from the i-th DG; $S_{rated,i}$ represents the rated apparent power output for the i-th DG.

IV. Proposed Control Strategy

The proposed frequency/active power controller is defined as:

$$\omega_i = \omega^* - m_i(P_i - P_i^*) + \Omega_i' \tag{3a}$$

$$\Omega_i' = \Omega_i - m_i P_i^* \tag{3b}$$

$$k_i \frac{d\Omega_i}{dt} = -(\omega_i - \omega^*) - \sum_{j=1}^{n} a_{ij}(\Omega_i - \Omega_j) \tag{3c}$$

where Ω_i' is the modified frequency/phase secondary control variable and Ω_i is the original frequency/phase secondary control variable; k_i is the frequency/phase secondary control gain; $A = \{a_{ij}\}$ presents the system communication topology: $a_{ij} = 1$ indicates a valid communication link between node i and node j and $a_{ij} = 0$ indicates no information exchange between node i and node j. In steady state, (1) $\omega_i = \omega^*$, meaning that system frequency is regulated to the nominal value; and (2) $\frac{P_i}{P_j} = \frac{m_j}{m_i} = \frac{S_{rated,i}}{S_{rated,j}}$, meaning that each DG supplies real power in proportion to its rating, regardless of its power output before islanding.

The proposed voltage/reactive power controller is defined as:

$$E_i = E^* - n_i(Q_i - Q_i^*) + e_i \tag{4a}$$

$$Q_i' = \frac{Q_i}{S_{rated,i}} \tag{4b}$$

$$\kappa_i \frac{de_i}{dt} = -\beta_i(E_i - E^*) - \sum_{j=1}^{n} b_{ij}(Q_i' - Q_j') \tag{4c}$$

where e_i is the voltage secondary control variable; κ_i is the voltage secondary control gain; β_i is the voltage magnitude regulation gain, $\beta_i = 1$ if i-th DG is selected to be voltage regulation DG otherwise $\beta_i = 0$; Q_i' is the normalized reactive power output of the i-th DG ; $B = \{b_{ij}\}$ is the adjacency matrix of system communication topology. In steady state, (1) $E_i = E^*$ for $\beta_i = 1$, meaning that voltage at i-th DG is regulated to the nominal value; and (2) $\frac{Q_i}{Q_j} = \frac{S_{rated,i}}{S_{rated,j}}$, meaning that each DG supplies reactive power in proportion to its rating, regardless of its power output before islanding.

When the proposed controllers are implemented, active power and reactive power sharing follows the conditions presented in (2). The proposed controller is an improvement over the approach presented in [7], [9], which proposed to implement a controller based on (3a), (3c) (4a), and (4c).This controller achieves precise frequency and voltage regulation while maintaining proportional active/reactive power sharing among all the DGs. However, the original controller is not designed for optimal apparent power utilization, since P^* and Q^* would vary in grid-connected mode. Our proposed control eliminates the offset introduces during grid-connected operation, to ensure that the conditions outlined in (2) are satisfied when the microgrid is islanded.

V. Distributed Algorithm Implementation

Equ. (3b)(3c) and (4b)(4c) are used to generate secondary control variables and would be implemented in RIAPS platform. Because of the nature of digital controller, the proposed controllers in (3b)(3c) and (4b)(4c) are first discretized:

$$\Omega_i'(k) = \Omega_i(k) - m_i {P_i}^* \tag{5a}$$

$$\Omega_i(k+1) = \Omega_i(k) + \frac{1}{k_i}[-(\omega_i(k) - \omega^*) - \sum_{j=1}^{n} a_{ij}(\Omega_i(k) - \Omega_j(k))] \times t \tag{5b}$$

$$Q_i'(k) = \frac{Q_i(k)}{S_{i\_Rate}} \tag{5c}$$

$$e_i(k+1) = e_i(k) + \frac{1}{\kappa_i}[-\beta_i(E_i(t) - E^*) - \sum_{j=1}^{n} b_{ij}({Q_i}'(k) - {Q'}_j(k))] \times t \tag{5d}$$

where t is the designed iteration time step.

According to (5) , local measurements ω, E, P^* and Q are needed in the secondary control algorithm. They are measured by individual DG and then sent to its associated RIAPS DG node. In RIAPS DG node, a RIAPS component **Sensor** will time stamp the measurements and pack them as local message **SensorData**. This local message is subscribed by a second RIAPS component **DistController** in the same node. RIAPS component **Sensor** and **DistController** together forms RIAPS actor **DGController**.

In **DistController** local measurement Q and local control variable Ω_k from the last time step will be packed as **NodeData** message together with timestamp and its IP address. **NodeData** will be published across the RIAPS network via a publish port. Furthermore, **DistController** has a subscribe port that subscribes **NodeData**. The publish-subscribe is handled by RIAPS broker of the platform. Therefore, component **DistController** can receive the **NodeData** messages as well.

As **DistController** is implemented on all the DG associated RIAPS nodes, each DG RIAPS node will publish a **NodeData** message containing its local measurement and control variable. At the same time, it will receive the **NodeData** messages of other nodes from the subscribe port. This is possible because RIAPS platform can distribute **DistController** component that runs concurrently in parallel on many nodes.

Every time step a clock port calls **DistController** to calculate the new control commands Ω_{k+1} and e_{k+1} using the equation (5). As a standard port in RIAPS, the time step of a clock port can be easily configured to best suit the algorithm. For voltage regulation DG, it only has the first term on the right of equation (5d) while all the other DGs only have the second term. If any **NodeData** message is not received in time, the values from the last time step will be used. After the new control variable Ω_{k+1} and e_{k+1} are calculated, they are sent to the the local DG to modify the droop curve. Ω_{k+1} is also packed into the **NodeData** to prepare for the next time step.

Besides the DG nodes, this application has a **Logger** node. It subscribes **NodeData** and display the data in real time. Also it stores the data in database for future use. Fig. 2 shows the proposed controller implementation in RIAPS platform.

VI. Simulation And Experiments Results

To validate the proposed control, the distributed microgrid apparent power control strategy is implemented on the RIAPS platform and tested on a real-time microgrid testbed, developed

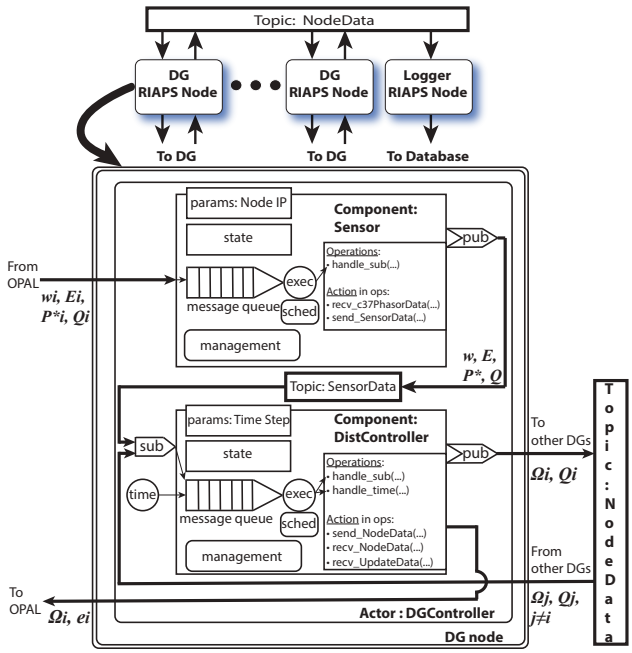

Fig. 2: RIAPS implementation of the proposed controller

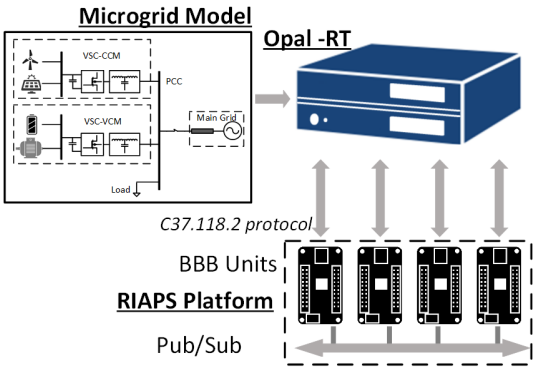

Fig. 3: Microgrid Hardware Testbed Setup

on the Opal-RT platform. Each DG is associated with a RIAPS Node, which is implemented on a BeagleBone Black (BBB) ARM Board. Since the DG inverter is simulated within the Opal-RT platform, the BBB units communicate with its respective DG via a communication link between the BBBs and the Opal-RT platform . IEEE C37.118.2 protocol is used for data transfer between Opal-RT and BBB units. The testbed setup is depicted in Fig.3.

A. Microgrid Testbed Specification

The microgrid topology is presented in Fig. 4 and the system parameters are presented in Table I. The controller parameters are designed based on the dynamic analysis done in [9]. Four DGs are implemented . All DGs are modeled as voltage source converter under voltage control mode (VSC-VCM). Loads are modeled as constant impedance loads. DG2 is selected to regulate the voltage. Droop control is implemented in all the DGs as the outer power loop. Each DG is linked to a single RIAPS node implemented in a beagle bone black (BBB). It is able to send out the measured real-time

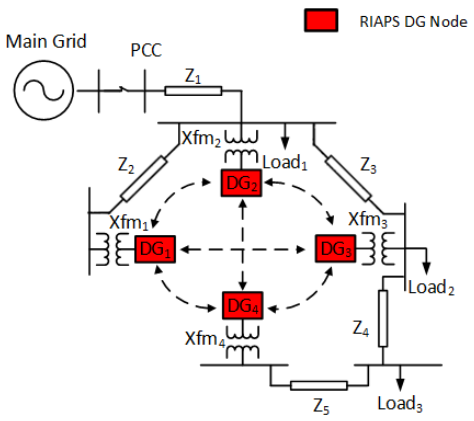

Fig. 4: Microgrid Topology

TABLE I: Microgrid System Parameters

DG Design	
DG_1	S_{rated}=250 kVA
$DG_{2,3,4}$	S_{rated}=100 kVA
Transmission Line Settings	
$z_1 = 0.045\Omega$, 14.3 mH	$z_2 = 0.11\Omega$, 3.56 mH
$z_3 = 0.14\Omega$, 2.27 mH	$z_4 = 0.24\Omega$ 7.48 mH
$z_5 = 0.16\Omega$, 5.05 mH	
Transformer Settings	
System Voltage Ratings	$V_{primary}$=13.2 kW $V_{secondary}$=480 V
Transformer 1	P_{rate}=300 kW X/R=3.5
Transformer 2,3,4	P_{rate}=112.5 kW X/R=2.1
Load Settings	
Load 1	P_{L1}=100 kW
Load 2	P_{L2}=200 kW
Load 3	P_{L3}=50 kW
Microgrid Synchronization Controller Design	
Frequency Control	$k = 5$
Voltage Control	$\kappa = 0.2$ $\beta = 0.02$
Iterative Step	t=100 ms

active/reactive power outputs to RIAPS DG Node and receive the updated secondary control variables from RIAPS DG Node at each iteration step, selected to be 100ms. Communication links between each DG are shown in Fig. 4 by dashed lines.

First, the controller presented in [9] is implemented. The simulation results are shown in Fig. 5. Microgrid is initially grid connected. All the DGs have non zero power reference under nominal frequency (P_1^*=0, P_2^*=35kW, P_3^*=20kW, P_4^*=10kW). The microgrid is islanded at t1 and the controller described in [9] is initiated at t2. When the steady-state is reached, the active power are not shared proportionally ($P_1 = 130kW$, $P_2 = 87kW$, $P_3 = 72kW$, $P_4 = 62kW$) while the reactive power is shared in proportion to the DG's power rating ($Q_1 = 11kVAR$, $Q_2 = Q_3 = Q_4 = 4.4kVAR$). In this case, the apparent power is not utilized optimally ($\frac{P_i}{Q_i} \neq \frac{P_j}{Q_j}$, $\left|\vec{S}_G\right| > \left|\vec{S}_L\right|$).

The proposed optimal apparent power control algorithm is implemented for comparison. The result are shown in Fig. 6. Microgrid is islanded at t1. At t2, the proposed controller is enabled. Active and reactive power generation among all the DGs are actively adjusted and re-distributed.

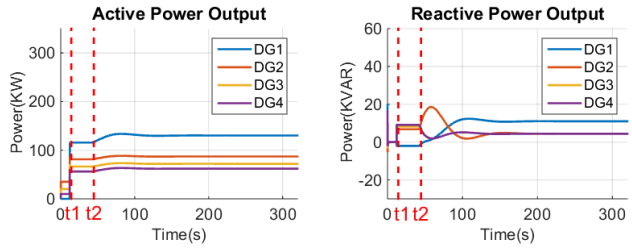

(a) Data Sets Collected in Opal-RT

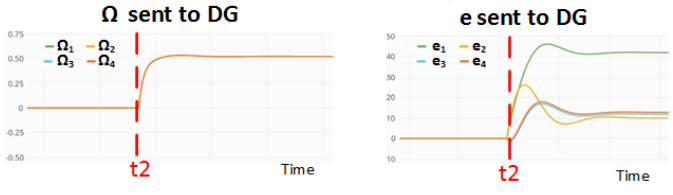

(b) Data Sets Collected in RIAPS Data Logger

Fig. 5: Simulation Results with Controller from [9]

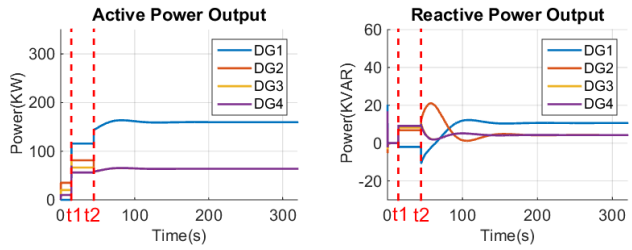

(a) Data Sets Collected in Opal-RT

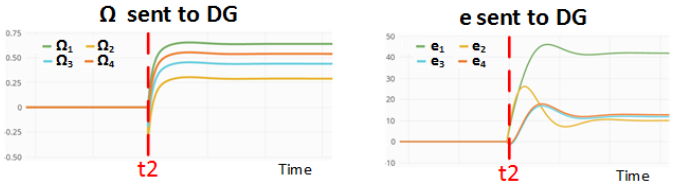

(b) Data Sets Collected in RIAPS Data Logger

Fig. 6: Simulation Results with Proposed Controller

In steady state, active and reactive power output of each DG is: $P_1 = 160kW$,$P_2 = P_3 = P_4 = 64kW$; $Q_1 = 10.5kVAR$, $Q_2 = Q_3 = Q_4 = 4.2kVAR$. Therefore, the optimal apparent power utilization conditions from (2) are met: $\frac{P_i}{Q_i} = 15.2$, for i=1,2,3,4; $\frac{P_1}{P_i} = \frac{Q_1}{Q_i} = 2.5 = \frac{S_{rated,1}}{S_{rated,i}}$ and $\frac{P_i}{P_j} = \frac{Q_i}{Q_j} = 1 = \frac{S_{rated,i}}{S_{rated,j}}$, for $i = 2, 3, 4$ and $i \neq j$.

VII. Conclusion

Optimal apparent power utilization in an islanded microgrid helps improve system resiliency, and mimimizes circulating ractive power flow. A distributed control algorithm is proposed in this paper based on the analysis of the apparent power distribution. The proposed control algorithm implements distributed averaging algorithm to ensure optimal apparent power utilization. It allows decoupled control on active and reactive power and optimal apparent power utilization in steady state. The proposed control algorithm is implemented in distributed local controllers using the RIAPS platform. Real time HIL simulation results show that the local controllers are able to optimally re-distribute apparent power flow within the islanded microgrid in a distributed manner. The authors are improving the proposed controller to be more robust against communication failure as future plan.

Acknowledgement This work was funded in part by the Advanced Research Projects Agency-Energy (ARPA-E), U.S. Department of Energy, under Award Number DE-AR0000666. The views and opinions of authors expressed herein do not necessarily state or reflect those of the US Government or any agency thereof.

References

[1] A. Bidram and A. Davoudi, "Hierarchical structure of microgrids control system," *IEEE Transactions on Smart Grid*, vol. 3, no. 4, pp. 1963–1976, 2012.

[2] A. Micallef, M. Apap, C. Spiteri-Staines, J. M. Guerrero, and J. C. Vasquez, "Reactive power sharing and voltage harmonic distortion compensation of droop controlled single phase islanded microgrids," *IEEE Transactions on Smart Grid*, vol. 5, no. 3, pp. 1149–1158, 2014.

[3] A. Kaur, J. Kaushal, and P. Basak, "A review on microgrid central controller," *Renewable and Sustainable Energy Reviews*, vol. 55, pp. 338–345, 2016.

[4] M. Savaghebi, A. Jalilian, J. C. Vasquez, and J. M. Guerrero, "Secondary control scheme for voltage unbalance compensation in an islanded droop-controlled microgrid," *IEEE Transactions on Smart Grid*, vol. 3, no. 2, pp. 797–807, 2012.

[5] J. Schiffer, R. Ortega, A. Astolfi, J. Raisch, and T. Sezi, "Conditions for stability of droop-controlled inverter-based microgrids," *Automatica*, vol. 50, no. 10, pp. 2457–2469, 2014.

[6] M. Yazdanian and A. Mehrizi-Sani, "Distributed control techniques in microgrids," *IEEE Transactions on Smart Grid*, vol. 5, no. 6, pp. 2901–2909, 2014.

[7] J. W. Simpson-Porco, F. Dörfler, and F. Bullo, "Synchronization and power sharing for droop-controlled inverters in islanded microgrids," *Automatica*, vol. 49, no. 9, pp. 2603–2611, 2013.

[8] G. Chen and E. Feng, "Distributed secondary control and optimal power sharing in microgrids," *IEEE/CAA Journal of Automatica Sinica*, vol. 2, no. 3, pp. 304–312, 2015.

[9] J. W. Simpson-Porco, Q. Shafiee, F. Dörfler, J. C. Vasquez, J. M. Guerrero, and F. Bullo, "Secondary frequency and voltage control of islanded microgrids via distributed averaging," *IEEE Transactions on Industrial Electronics*, vol. 62, no. 11, pp. 7025–7038, 2015.

[10] J. Kim, J. M. Guerrero, P. Rodriguez, R. Teodorescu, and K. Nam, "Mode adaptive droop control with virtual output impedances for an inverter-based flexible ac microgrid," *IEEE Transactions on Power Electronics*, vol. 26, no. 3, pp. 689–701, 2011.

[11] A. Milczarek, M. Malinowski, and J. M. Guerrero, "Reactive power management in islanded microgridproportional power sharing in hierarchical droop control," *IEEE Transactions on Smart Grid*, vol. 6, no. 4, pp. 1631–1638, 2015.

[12] H. Cai, R. Zhao, and H. Yang, "Study on ideal operation status of parallel inverters," *IEEE Transactions on Power Electronics*, vol. 23, no. 6, pp. 2964–2969, 2008.

[13] G. A. Agha, "Actors: A model of concurrent computation in distributed systems." MIT Cambridge Artificial Intelligence Lab, Tech. Rep., 1985.

[14] S. Eisele, I. Madari, A. Dubey, and G. Karsai, "Riaps: resilient information architecture platform for decentralized smart systems," in *20th IEEE International Symposium On Real-Time Computing, IEEE. Toronto, Canada: IEEE*, vol. 5, 2017, p. 2017.